Coupling Between Vehicle Motion and Slender Cone Transition

L. E. Ericsson*
Lockheed Missiles & Space Company, Inc., Sunnyvale, California

An analysis has been performed of the existing experimental evidence of the coupling existing between vehicle motion and the slender cone boundary-layer transition. It is found that, on the leeward side, the transition effects are important only in relation to the in-plane aerodynamics, whereas the opposite is true on the windward side where the important transition effects are limited to the out-of-plane aerodynamics.

Nomenclature

D = maximum diameter
ℓ = body length
m = pitching moment, coefficient $C_m = m/(\rho_\infty U_\infty^2/2)SD$
M = Mach number
n = yawing moment, coefficient $C_n = n/(\rho_\infty U_\infty^2/2)SD$
N = normal force, coefficient $C_N = N/(\rho_\infty U_\infty^2/2)S$
p = spin rate
P = static pressure, coefficient $C_p = (P-P_\infty)/(\rho_\infty U_\infty^2/2)$
Re = Reynolds number, $Re = U_\infty \ell/\nu_\infty$
S = reference area, $S = \pi D^2/4$
t = time
U = velocity
x = axial distance from nose tip
α = angle of attack
β = angle of side slip
Δ = increment or amplitude
θ = perturbation in pitch
θ_c = cone half-angle
ν = kinematic viscosity of air
ρ = air density
σ = total flow inclination, $= (\alpha^2+\beta^2)^{1/2}$
ϕ = body azimuth
ϕ_R = orientation of moment asymmetry
ψ = precession angle

Subscripts

b = base
B = body fixed
CG = center of gravity
max = maximum
TR = transition
w = wall
∞ = freestream

Superscript

i = transition-induced, e.g., $\Delta^i C_N$

Derivative Symbols

$C_{m\alpha} = \partial C_m/\partial\alpha$
$C_{m\dot\theta} = \partial C_m/\partial(\dot\theta D/U_\infty)$
$C_{\dot m\dot\theta}$ = integrated mean value, $= C_{mq} + C_{m\dot\alpha}$
$C_{np} = \partial C_n/\partial(pD/2U_\infty)$
$C_{np\alpha} = \partial C_{np}/\partial\alpha$
$\dot\theta = \partial\theta/\partial t$

Introduction

WHEN the boundary-layer transition moves up over the base of a slender re-entry body, the effects on the vehicle's dynamics can be large: i.e., on an ablating body, the loss of dynamic stability in pitch or yaw may result.[1] On the other hand, on a nonablating vehicle, the boundary-layer transition has a favorable effect on the dynamic stability in pitch, as has been shown by Ward[2] for a 10 deg pointed cone (see Fig. 1). The reason for this is that the boundary-layer crossflow causes a forward transition movement on the leeward side, generating a negative normal force on the aft body[2] (Fig. 2). The corresponding effect on the static stability is destabilizing. However, because of the crossflow time lag effects, the corresponding effect on the dynamic stability is stabilizing,[3,4] in agreement with the experimental results shown in Fig. 1.

It was shown in Ref. 3 that if the transition front is represented by a straight line (see Fig. 2), the difference in the displacement surface slopes for laminar and turbulent boundary layers produces a negative normal force that gives a statically destabilizing moment contribution in good agreement with the one measured experimentally.[2] For the 1.8 deg oscillation amplitude used in the dynamic test, the main transition-induced effect comes from the leeward side[3] (Fig. 3), as can be expected from the experimental results shown in Fig. 2. When the mean transition location moves forward of the oscillation center, $x_{CG}/\ell = 0.55$, the transition-induced effect changes sign.[3] It can be seen that, for the amplitude $\Delta\theta/\theta_c = 0.18$, the maximum transition-induced damping occurs when the transition at $\alpha = 0$ occurs half a body length aft of the base. That is, only the leeward side transition effects are present.

Thus, for pure oscillations in pitch, only the transition effects on the leeward side are of any significance. However, for body spin and/or coning, the windward side effects can become the dominant ones.

Discussion

Figure 4 shows flight test results for the variation with time of the total angle of attack (σ) of a slender cone.[5,6] At the time of "transition" marked in the figure, flight instrumentation showed the transition to occur both on the forebody (leeside transition) and the aft body (windward transition). Thus, before the "transition" in Fig. 4, only the leeside transition effects are likely to have been important.

Presented as Paper 86-1823 at the AIAA Fourth Applied Aerodynamics Conference, San Diego, CA, June 9-11, 1986; received June 24, 1986; revision received Oct. 27, 1986.

*Senior Consulting Engineer. Fellow AIAA.

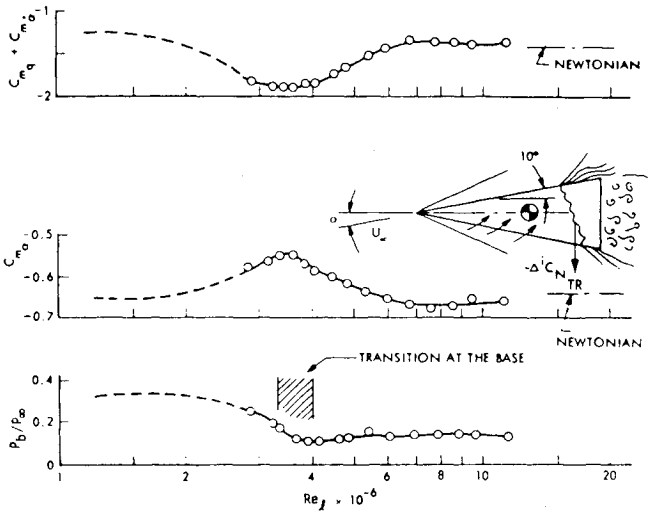

Fig. 1 Effect of transition on the aerodynamic characteristics of a 10 deg sharp cone at $M_\infty = 5$, $\alpha = 0$, with $\Delta\theta = 1.8$ deg (from Ref. 2).

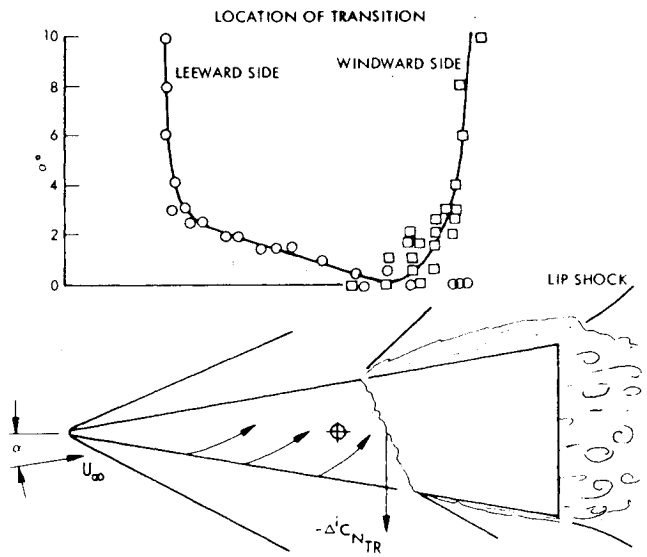

Fig. 2 Effect of angle of attack on transition geometry on a 10 deg sharp cone at $M_\infty = 5$, $Re = 8 \times 10^6$ (from Ref. 2).

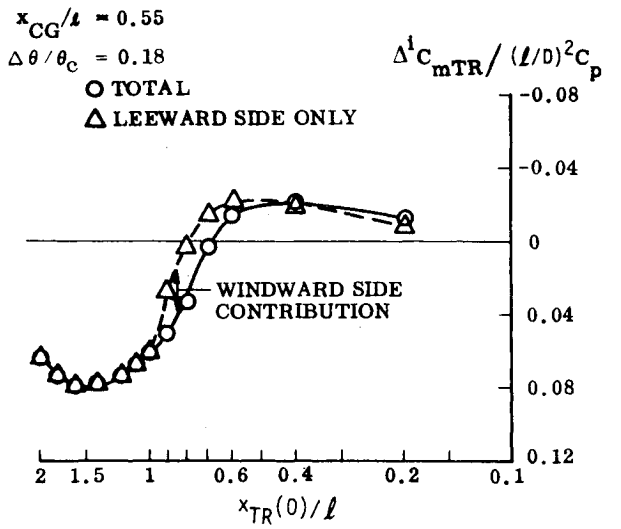

Fig. 3 Effect of transition location on the induced incremental pitching moment at small angles of attack (from Ref. 3).

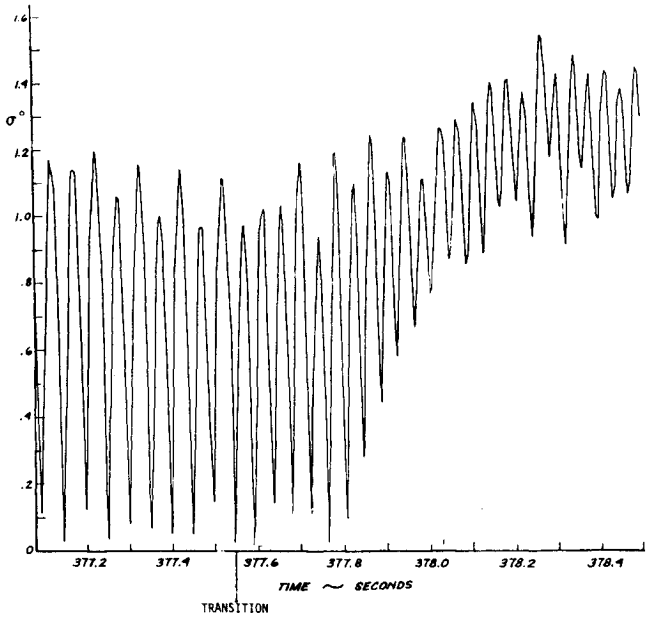

Fig. 4 Hypersonic full-scale free flight attitude response to transition on a slender cone (from Ref. 6).

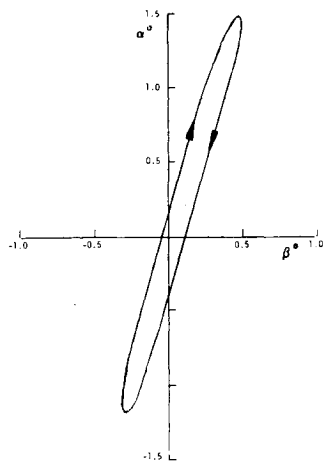

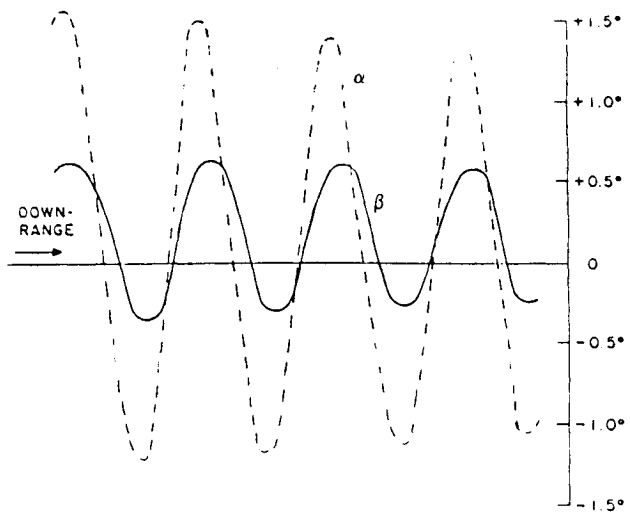

Fig. 5 Ballistic range free flight response to transition on a 5 deg sharp cone at $M_\infty = 5$ (from Ref. 7).

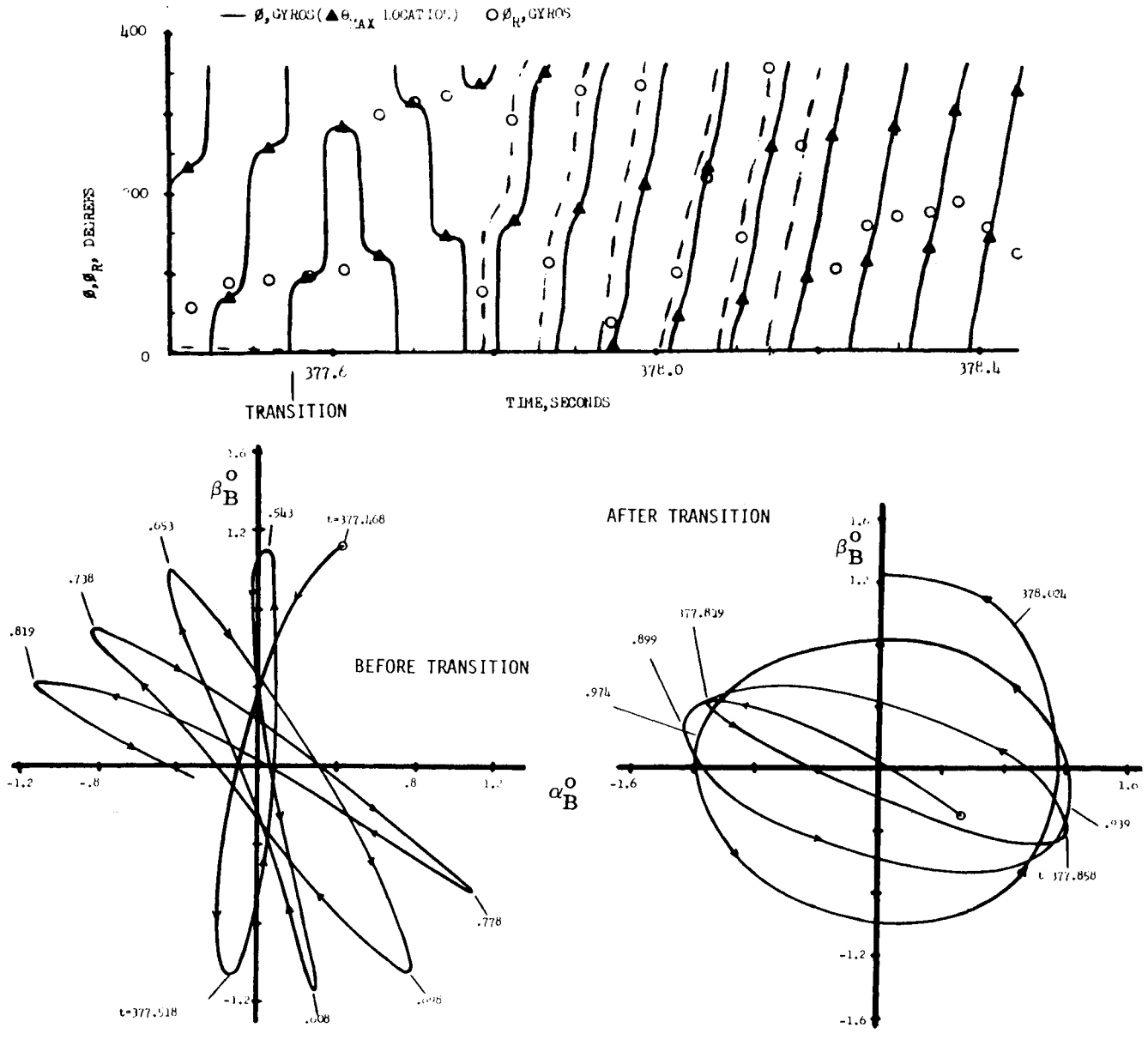

Fig. 6 Effect of transition on free flight motion behavior of a slender cone at hypersonic speeds (from Ref. 5).

This explains the initially damped behavior of the σ oscillations, similar to what has been observed by Sheetz[7] in ballistic range tests (Fig. 5). The recorded motion history "before transition"[5,6] (Fig. 6) is of the precessing planar type, in agreement with what is expected for the case where the leeside transition effects dominate. However, "after transition," the motion behavior changes from precessing planar to the coning type.[5,6] See Fig. 6. How this is the result of the so-called "moving wall" effects on the windward side boundary-layer transition will be discussed in the next section.

Moving Wall Effects

Experiments with a rotating cylinder, aligned axially with the freestream velocity, show that transition is promoted by body spin.[8] (See Fig. 7a.) At angle of attack, the spin-induced promotion of transition is amplified greatly on the side where the spin-induced velocity opposes the α-induced crossflow ($180<\phi<360$ deg in Fig. 7b), whereas the transition is delayed on the opposite side, where wall velocity and crossflow act in the same direction ($0<\phi<180$ deg in Fig. 7b). Tests with an ogive-cylinder body at $\alpha=0$ and 6 deg demonstrate how powerful the spin-induced transition-promotion can be.[9] (See Fig. 8.) At $\alpha=6$ deg, the Reynolds number and wall velocity need be only a fraction of what they are at $\alpha=0$ to produce the earliest occurrence of transition at the same axial station.

Sturek[10,11] has performed systematic supersonic tests with a 10 deg sharp cone to determine the effect of body spin on the transition geometry at angle of attack. The definition of the transition geometry at $M=2$ and $\alpha=4$ deg is shown in Fig. 9 for zero spin. The present author has modified the leeside fairing to agree better with the experimental results. Figure 10 shows the effect of spin rate on the transition geometry. As for the spinning ogive cylinder in Fig. 8, the windward side transition is promoted by the effect of the upstream-moving wall and the leeside transition is delayed by the downstream-moving wall effect. In addition, Fig. 10 shows that spin has little effect on the leeside transition geometry. This is to be expected, as the boundary layer is much thicker on the leeward than on the windward side. Thus, the relative effect of the wall velocity is small, becom-

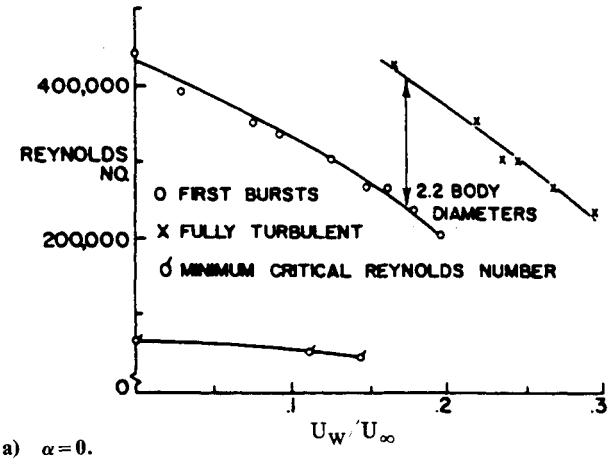

a) $\alpha = 0$.

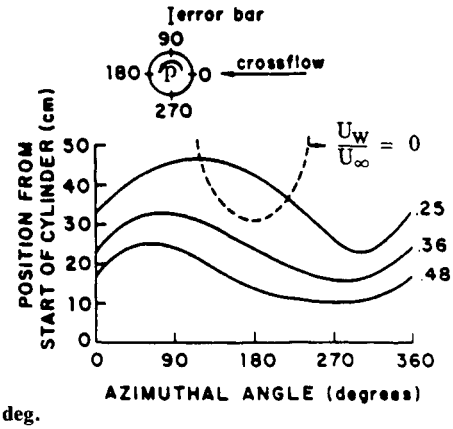

b) $\alpha = 3$ deg.

Fig. 7 Effect of spin on low speed transition on a circular cylinder shell (from Ref. 8).

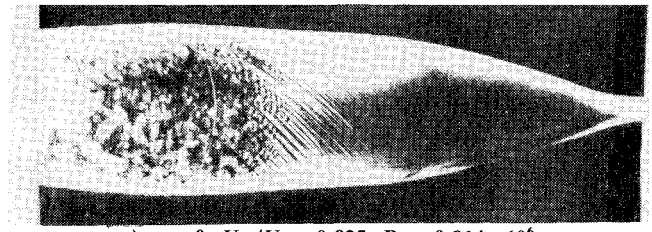

a) $\alpha = 0$, $U_w/U_\infty = 0.825$, $Re_\ell = 0.814 \times 10^6$.

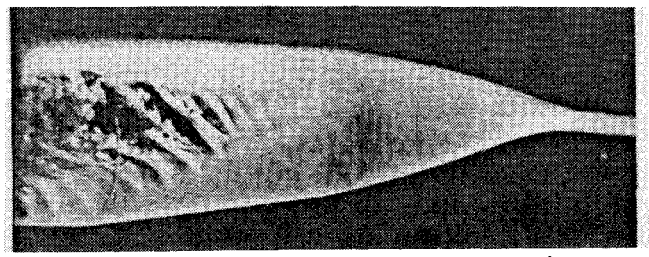

b) $\alpha = 6$ deg, $U_w/U_\infty = 0.169$, $Re_\ell = 0.315 \times 10^6$.

Fig. 8 Smoke flow visualization of low-speed transition on a spinning ogive-cylinder, side view (from Ref. 9).

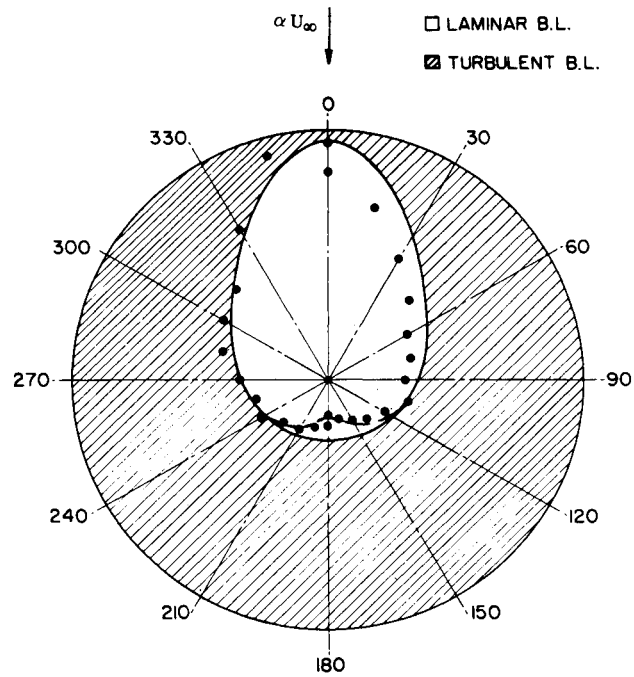

Fig. 9 Transition geometry on a sharp 10 deg cone at $M_\infty = 2$ and $Re = 5.97 \times 10^6$ (from Ref. 10).

ing increasingly so as the nose tip is approached. Whereas the crossflow maintains the same magnitude, the moving wall velocity decreases with the decreasing body radius as the nose is approached.

Consequently, one can generalize in regard to the transition on a spinning body. On the leeward side, the dominant influence on the boundary-layer transition is the α-generated crossflow, whereas the spin-induced wall velocity dominates on the windward side.

The moving wall effects for spinning and coning bodies are somewhat similar. See Fig. 11. Instead of being constant, as in the spinning case, the moving wall velocity varies around the periphery of the coning body. The maximum wall velocity $|U_w|_{max}$ occurs on the top and bottom meridians, with only the latter case being of importance. At supersonic speeds, the transition bulge will generate a side force that drives the coning motion. This proconing effect is present until the centroid of the windward side transition has moved to the center of gravity. As the relative side slip angle ($|U_w|_{max}/U_\infty$) due to coning generates inviscid pressure forces that act against the coning motion, one can expect a build-up to a limit cycling motion. This is exactly the behavior observed in flight of a slender blunted cone.[5,6] See Fig. 6. When transition occurs on the windward side of the body, the (α,β) plot shows a change to the coning type of motion behavior described by Fig. 11b. The aerodynamic asymmetry changes from the transient, body-fixed type described in Refs. 5 and 6 to the transition-induced wind-fixed one shown in Fig. 11. This is illustrated by the results in the top graph of Fig. 6, where the "body-fixed" asymmetry starts rotating relative to the body after $t = 377.8$ s.

In free flight, a slender vehicle usually spins during its coning motion. The moving wall effects generated by spin and coning are different and the corresponding transition-induced effects are, therefore, also different. Figure 12 shows how the Magnus moment α derivative ($C_{np\alpha}$), measured on a 10 deg cone, varies as boundary-layer transition moves forward from the base.[12] The spin-induced moving wall velocity decreases linearly with the distance from apex, whereas the transition-induced yawing moment is proportional to the distance to the c.g. and, consequently, changes sign when transition moves forward of the c.g. The difference in regard to the coning motion is that the moving wall velocity is proportional to the distance from the c.g., not the distance from the apex. This causes the transition-induced yawing moment to be proportional to the square of the transition distance to the c.g. Consequently, there is no change in sign of the moment when transition moves forward of the c.g. The transition-induced moment continues to be of proconing nature, after having dipped to zero when the windward side transition is centered around the c.g.

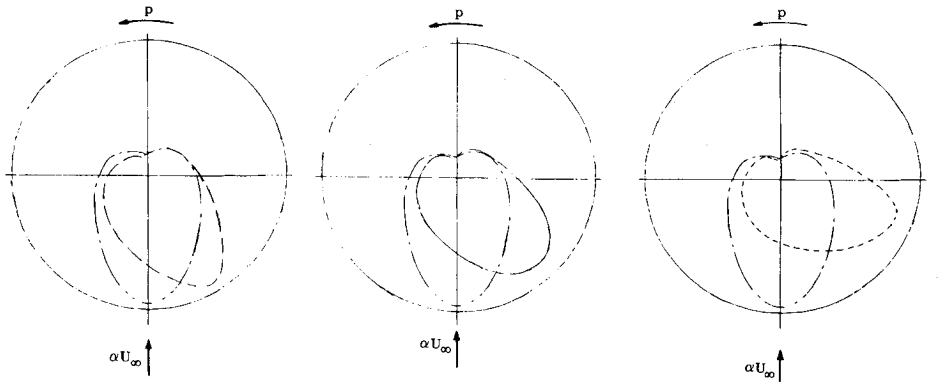

a) $pD/2U_\infty = 0$ and 0.06. b) $pD/2U_\infty = 0$ and 0.12. c) $pD/2U_\infty = 0$ and 0.18.

Fig. 10 Effect of spin on the transition geometry of a 10 deg sharp cone at $M_\infty = 2$ and $Re = 5.97 \times 10^6$ (from Ref. 10).

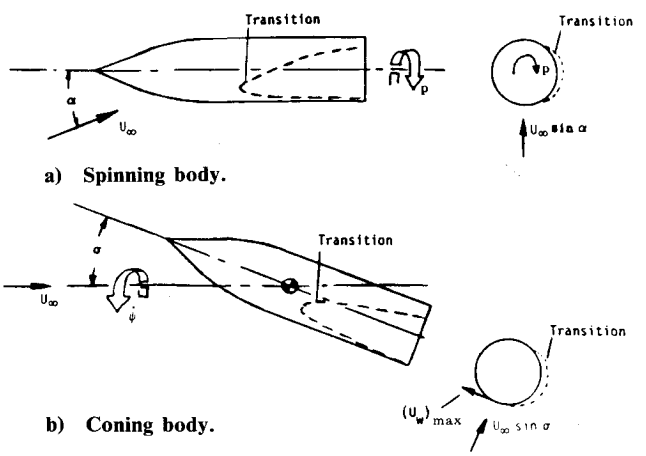

Fig. 11 Conceptual moving wall effects on transition for a slender body in spinning or coning motion.

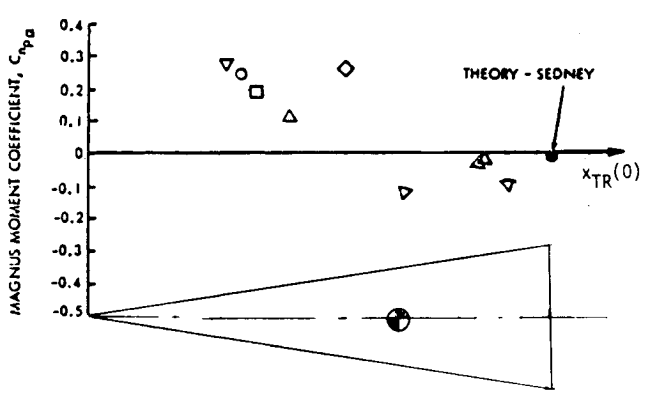

Fig. 12 Effect of transition on the Magnus moment derivative of a 10 deg sharp cone at $M_\infty = 2.5$ (from Ref. 12).

In the preceding discussion, the results obtained in ground tests with nonablating models have been compared with flight test data for an ablating slender cone[5,6] (Figs. 4 and 6). It is well known that the effect of ablation and associated time lag on vehicle dynamics can be large.[1,13] However, the extensive analysis in Refs. 5 and 6 of several flight vehicles led to the conclusion that, whereas ablation may have augmented the transition effects, the physical mechanism generating the observed vehicle motion was related to transition itself rather than to the ablation process.

Conclusions

An analysis of available experimental results has led to the following conclusions in regard to the coupling between vehicle motion and slender cone boundary-layer transition:

1) When transition first occurs on the vehicle, only the leeward side effects are important, generating statically destabilizing but dynamically stabilizing effects on the planar motion characteristics.

2) When transition starts occurring also on the windward side, it will produce a change from precessing planar to coning motion of limit cycle character.

3) The leeward side transition effects are reversed when transition moves forward of the center of gravity. However, the windward side transition effects do not change sign, but remain proconing in character.

References

[1]Ericsson, L. E. and Reding, J. P., "Ablation Effects on Vehicle Dynamics," *Journal of Spacecraft and Rockets*, Vol. 3, Oct. 1966, pp. 1476–1483.

[2]Ward, L. K., "Influence of Boundary-Layer Transition on Dynamic Stability at Hypersonic Speeds," *Transactions of the Second Technical Workshop on Dynamic Stability Testing*, Vol. II, Arnold Engineering Development Center, Arnold Air Force Station, TN, Paper 9, April 1965.

[3]Ericsson, L. E., "Effects of Boundary Layer Transition on Vehicle Dynamics," *Journal of Spacecraft and Rockets*, Vol. 6, Dec. 1969, pp. 1404–1409.

[4]Ericsson, L. E., "Transition Effects on Slender Vehicle Stability and Trim Characteristics," *Journal of Spacecraft and Rockets*, Vol. 11, Jan. 1974, pp. 3–11.

[5]Chrusciel, G. T., "Analysis of R/V Behavior during Boundary Layer Transition," AIAA Paper 74-109, Jan. 1974.

[6]Chrusciel, G. T., "Analysis of Reentry Vehicle Behavior during Boundary Layer Transition," *AIAA Journal*, Vol. 13, Feb. 1975, pp. 154–159.

[7]Sheetz, N. W. Jr., "Free-Flight Boundary Layer Transition Investigation at Hypersonic Speeds," AIAA Paper 65-127, Jan. 1965.

[8]Morton, J. B., Jacobson, I. D., and Saunders, S., "Experimental Investigation of the Boundary Layer on a Rotating Cylinder," *AIAA Journal*, Vol. 14, Oct. 1976, pp. 1458–1463.

[9]Kegelman, J. T., Nelson, R. C., and Mueller, T. J., "Boundary Layer and Side Force Characteristics of a Spinning Axisymmetric Body," AIAA Paper 80-1584, Aug. 1980.

[10]Sturek, W. B., "Boundary Layer Studies on a Spinning Cone," Ballistic Research Labs., Rept. R1649, May 1973.

[11]Sturek, W. B., "Boundary Layer Distortion on a Spinning Cone," *AIAA Journal*, Vol. 11, March 1973, pp. 395–396.

[12]Regan, F. J., "Magnus Effects," AGARD CP-10, Sept. 1966, pp. 341–364.

[13]Waterfall, A. P., "Effect of Ablation on the Dynamics of Spinning Re-Entry Vehicles," *Journal of Spacecraft and Rockets*, Vol. 6, Sept. 1969, pp. 1038–1044.